MINERALOGICAL MAGAZINE, SEPTEMBER 1973, VOL. 39, PP. 271–81.

The crystal structure of julgoldite

RUDOLF ALLMANN
Fachbereich Geowissenschaften, Philipps-Universität, 355 Marburg, Germany

AND GABRIELLE DONNAY
Department of Geological Sciences, McGill University, Montreal 101, Quebec, Canada

SUMMARY. The structure of julgoldite, $Ca_2(Fe^{2+}_{1-x}Fe^{3+}_x)Fe^{3+}_2Si_3O_{10+x}(OH)_{4-x}(x \approx 0{\cdot}5)$, has been determined and refined to an R value of 4·6 % based on 2417 symmetry-independent reflections, of which 765 are unobserved (weighted $R = 4{\cdot}3$ %). The cell dimensions are a 8·922(4), b 6·081(3), c 19·432(9) Å, β 97·60(6)°, the space group is $A2/m$ with $Z = 4$ and D_{calc} 3·56 g cm^{-3}. Julgoldite is isostructural with pumpellyite; the Si–O and Ca–O distances of julgoldite are identical, within experimental accuracy, with corresponding distances in pumpellyite; the Fe–O distances of julgoldite are about 0·09 Å longer than the corresponding (Al, Mg)–O distances in pumpellyite. The four hydroxyl groups and the extent of O-for-OH substitution are identified by valence-sum calculations.

PUMPELLYITE, for which the formula $Ca_2Al_2(OH)_2(Al_{0{\cdot}5}Mg_{0{\cdot}5})(OH, O)SiO_4.Si_2O_6(OH, O)$ has recently been proposed (Allmann and Donnay, 1971), has become a mineral of special interest because of its role in low-grade metamorphism (see, for example, Coombs, 1961). In the absence of good-quality single crystals, Galli and Alberti (1969) were unable to obtain the high-quality intensity data that are a prerequisite for structure refinement. The 793 visually estimated intensities, 205 of which were unobserved, led to $R = 15{\cdot}9$ %, and the 588 observed reflections to $R = 12{\cdot}3$ %. Refining the pumpellyite structure type became possible when Moore (1971) described an iron analogue of pumpellyite, the new mineral julgoldite, $Ca_2(Fe^{2+}_{1-x}Fe^{3+}_x)Fe^{3+}_2Si_3O_{10+x}(OH)_{4-x}$, from Långban, Sweden. Professor Moore kindly gave us crystals on which to work. Julgoldite crystals are of good quality and thus afford an accurate structure determination.

Crystal description and crystal data. A small portion ($\approx$ 0·3 g) of a specimen from Långban, Sweden, contained several shiny black plates of julgoldite embedded in clear apophyllite. In addition we noted a small aggregate of tiny dull-black crystals; they were at first mistaken for julgoldite, but, on the basis of a microprobe analysis (see below), they are probably ilvaite, $CaFe^{2+}_2Fe^{3+}(OH)OSi_2O_7$.

A crystal was first mounted along b and used for the measurement of lattice constants and intensities hol–$h9l$: it is a (100) plate, in the shape of an isosceles trapezium, which has two edges parallel to b, with lengths 0·44 and 0·23 mm; the height along c is 0·29 mm and the thickness along a^* is 0·06 mm. The same plate was then mounted parallel to the a axis to measure the okl reflections. The cell dimensions, measured with Mo-$K\alpha_1$ radiation (λ 0·70926 Å) have the following values at 20 °C: a 8·922(4), b 6·081(3), c 19·432(9) Å, β 97·60(6)°, V = 1044 Å^3, with space group $A2/m$, $Z = 4$.

D_{calc} 3·56 g cm^{-3}. We had too little material to remeasure the density, for which Moore (1971) reported the value D_{obs} 3·602 g cm^{-3}. His sample may have contained admixed ilvaite, whose reported density ranges from 3·8 to 4·1 g. cm^{-3}: this would account for the high measured value.

Crystal chemistry. A few hand-picked crystals of julgoldite were submitted to Dr. K. Abraham (Ruhr-Universität, Bochum) for a microprobe analysis on his Microscan V instrument run at 20 KeV, 30 nA. His results (table I, columns *c* and *d*) show reasonably good agreement with the theoretical composition given above for julgoldite (table I, *a*), except that about 5 atomic % of Fe^{3+} is replaced by Al

TABLE I. *Electron-microprobe analyses of julgoldite and associated mineral from Långban, Sweden*

	a	*b*	*c*	*d*	*e*	*f*	*g*	*h*
SiO_2	32·2	32·4	32·4	31·0–32·0	34·0	34·0	26·8	29·3
TiO_2	—	—	—	—	0·1	—	—	—
Al_2O_3	—	1·1	1·0	1·0–1·9	1·3	1·0	—	—
Fe_2O_3	35·7	34·1	—	—	29·6	31·4	—	19·6
FeO	6·4	6·5	—	—	8·7	6·0	—	35·2
ΣFe as Fe_2O_3	(42·8)	(41·3)	40·6	39·9–41·4	(39·3)	(38·1)	59·7	(58·7)
CaO	20·1	20·2	19·3	19·3–20·0	22·0	20·6	13·6	13·7
MnO	—	—	—	—	0·2	—	0·2	—
MgO	—	—	—	—	0·2	—	—	—
BaO	—	—	—	—	0·01	—	—	—
H_2O	5·6	5·7	not detd.	not detd.	4·69	6·5	not detd.	2·2
Total	100·0	100·0	93·3*	91·8–93·6*	100·7	100·0†	100·3*	100·0

Microprobe analyses by Dr. K. Abraham; emission spectrographic analysis by B. Rajandi; iron oxidation grade and water determination by P. Moore (Moore, 1971).

a. Theoretical composition for $Ca_2Fe^{3+}_{2.5}Fe^{2+}_{0.5}Si_3O_{10.5}(OH)_{3.5}$.
b. Theoretical composition for $Ca_2(Fe^{2+}_{0.5}Fe^{3+}_{0.5})(Fe^{3+}_{1.875}Al_{0.125})Si_3O_{10.5}(OH)_{3.5}$.
c. Microprobe analysis of a nearly homogeneous area in one julgoldite specimen.
d. Microprobe analyses of numerous points on four different crystals.
e. Emission spectrographic analysis from Moore, 1971.
f. Theoretical composition as given under *b* with the addition of 8 wt % apophyllite.
g. Microprobe analysis of one crystal of associated mineral. Sum too high, because all Fe is taken to be Fe^{3+}.
h. Theoretical composition of ilvaite, $CaFe^{2+}_2Fe^{3+}(OH)OSi_2O_7$.

* H_2O not determined. † Including 0·5 % KF.

(Table I, *b*). All crystals were observed to be somewhat inhomogeneous, especially in Al content, which ranged from 0 to 1·5 wt %; Ca was nearly constant; Fe and Si showed small variations with negative correlation; Mn, Mg, Ti, K, Na, Cr, Ni, and Zn were looked for, but were not detected.

The observed range of the Al content is in line with a composition intermediate between julgoldite and pumpellyite, which is cited by Moore (1971); the three Fe atoms per formula unit of stoichiometric julgoldite are here replaced by

($Fe^{3+}_{1\cdot17}Al_{1\cdot03}Fe^{2+}_{0\cdot66}\square_{0\cdot03}$). The possibility of a complete solid solution, with $Fe^{3+}_{2\cdot5}Fe^{2+}_{0\cdot5}$ and $Al_{2\cdot5}Mg_{0\cdot5}$ representing the end-member contents in the two variable cation positions was already mentioned by Moore.

The emission spectrographic analysis of julgoldite performed by Benita Rajandi (Moore, 1971) is high in SiO_2 and CaO (table I, *e*). This fact could easily be due to a slight contamination of the sample with apophyllite, in which the julgoldite crystals are embedded: 8 wt % of admixed apophyllite would account for the reported results (table I, *f*).

The oxidation state of the iron as determined by P. Moore (table I, *e*) is high in Fe^{2+} when compared with the rather low H_2O content. We fixed the occupancy of Fe(2) at ($Fe^{2+}_{0\cdot5}Fe^{3+}_{0\cdot5}$) by crystallochemical considerations (mainly on the basis of the differences in distances Fe(1)–O and Fe(2)–O, see table V). But the Fe^{2+} content may well vary somewhat depending on the O_2 partial pressure at the time of formation. The excess Fe^{2+} from Moore's analysis could be accounted for by associated ilvaite, whose structure is very similar to that of julgoldite. Crystals from the dull-black aggregate that is associated with julgoldite were also studied by Dr. Abraham (table I, *g*). They fit the description of one of the two unidentified phases described by Moore (1971). They contain no Al, but 0·2 wt % MnO. The agreement with the theoretical composition of ilvaite (table I, *h*) is quite acceptable.

Structure determination. Intensities were collected on an automated two-circle goniometer with Zr-filtered Mo-$K\alpha$ radiation out to a maximum $(\sin\theta)/\lambda$ value of 0·8 $Å^{-1}$. The linear absorption coefficient is 55·8 cm^{-1}, so that absorption corrections could be considered negligible for the above crystal. As can be seen in table III, the final B_{11} values are on the average about 0·26 $Å^2$ larger and the B_{33} values about 0·27 $Å^2$ smaller than the average B values, mainly due to the missing absorption correction of the platy crystal set along *b*. The o*k*o reflections were taken from the zero layer of the crystal, set along *a*. Of the 2417 symmetry-independent reflections that were measured,[1] 765 were too weak to be observed and were given an F_{obs} value of zero. Intensities were corrected for Lorentz and polarization factors.

The layers with *k* odd ($\approx$ 40 % unobserved reflections) are much weaker than the layers with *k* even ($\approx$ 24 % unobserved reflections). As the Fe atoms are contributing little to the weak layers, the intensities of these are very similar to those of pumpellyite (Galli and Alberti, 1969), since all atoms are the same in julgoldite as in pumpellyite, except for Fe, which takes the place of Al and (Al, Mg).

Starting with the atomic parameters of pumpellyite (R = 8·6 %), the refinement quickly dropped to a conventional residual of R = 6·2 % with isotropic temperature factors. The atomic form factors used for Fe^{3+}, Ca^{2+}, and O^- were those of Hanson and Pohler (1966), and the one for SiO comes from Hanson *et al.* (1964). Then Cromer's (1965) correction terms for anomalous dispersion were applied to the form factors of the cations. The temperature factors did change somewhat (see Table II), but the R value did not. After introduction of anisotropic temperature factors and anomalous

[1] Most reflections were measured twice. The symmetry-related intensities varied less than 10 %, except for some weak reflections.

dispersion correction as above, R further decreased to 4·6 %. The corresponding weighted R value is 4·3 %. In the last cycle all but five of the 765 unobserved reflections had F_{calc} values smaller than the assumed F_{min} value of 22. For all unobserved reflections with $F_{calc} < F_{min}$, the difference $F_{calc}-F_{obs}$ was set equal to zero. Thus the unobserved reflections, except the five mentioned above, do not contribute to the R values, but their derivatives are included in the calculation of the parameter shifts. $\sigma(F_{obs})$ was taken as $(0{\cdot}67\ F^2_{min}+0{\cdot}03\ F^2_{obs})/F_{obs}$ for the observed reflections and as F_{min} for the unobserved ones.[1]

TABLE II: *Julgoldite. Final fractional coordinates with standard deviations (at $R = 4{\cdot}6$ %) and two sets of isotropic temperature factors (at $R = 6{\cdot}2$ %). $\bar{\sigma}$ is the absolute standard deviation averaged over the two or three varied coordinates*

Atom	x	y	z	$\bar{\sigma}$	B*	B†	Point position
Ca(1)	0·2554(2)	½	0·3397(1)	2.10^{-3} Å	0·43 Å²	0·47 Å²	4(i)
Ca(2)	0·1963(3)	½	0·1563(1)	2	0·74	0·78	4(i)
Fe(1)	½	¼	¼	—	0·67	0·75	4(f)
Fe(2)	0·2543(1)	0·2465(2)	0·4955(·5)	1	0·48	0·55	8(j)
Si(1)	0·0506(3)	0	0·0936(1)	3	0·33	0·34	4(i)
Si(2)	0·1623(3)	0	0·2478(1)	3	0·41	0·42	4(i)
Si(3)	0·4650(3)	0	0·4013(1)	3	0·30	0·30	4(i)
O(1)	0·1353(6)	0·2214(9)	0·0755(2)	5	0·76	0·72	8(j)
O(2)	0·2582(5)	0·2292(9)	0·2473(2)	5	0·72	0·69	8(j)
O(3)	0·3674(6)	0·2192(9)	0·4135(2)	5	0·86	0·81	8(j)
O(4)	0·1283(8)	½	0·4428(4)	7	0·52	0·47	4(i)
O(5)H	0·1234(9)	0	0·4556(4)	8	1·06	1·01	4(i)
O(6)	0·3717(8)	½	0·0453(4)	7	0·55	0·52	4(i)
O(7)H	0·3757(9)	0	0·0332(4)	8	1·07	1·02	4(i)
O(8)	0·0315(9)	0	0·1780(4)	7	0·79	0·75	4(i)
O(9)	0·4728(8)	½	0·1746(4)	7	0·56	0·52	4(i)
O(10)H	0·0615(9)	0	0·3128(4)	8	1·04	0·98	4(i)
O(11)H	0·4974(9)	0	0·1835(4)	8	0·93	0·88	4(i)

* Without anomalous dispersion correction.
† With anomalous dispersion correction.

The final atomic coordinates and isotropic temperature factors are listed in table II; the anisotropic temperature factors are shown in table III. The final coordinates and our cell dimensions were used by Mrs. E. Evans, of the National Bureau of Standards, Washington, D.C., to calculate spacings and intensities of the theoretical julgoldite powder pattern for comparison with the experimental pattern of Moore (table IV).

Discussion of the structure. The julgoldite structure is best viewed down its b axis, projected onto the ac plane (fig. 1). The slight differences between it and the pumpellyite structure are due to the different sizes of the octahedral cations. Bond lengths

[1] A table of F_{obs} F_{calc} has been deposited in the library of the Dept. of Mineralogy, British Museum (Natural History), London SW 7; copies may be obtained on request.

and bond valences, to be discussed below, are summarized in table V; table VI gives the lengths of the edges of all coordination polyhedra and the angles they subtend at their central cation, as well as the cation–cation distances less than 3·3 Å.

The octahedra form chains along *b* by sharing opposite edges. They are of two kinds: Fe(1), which makes up one-third of the total iron content, is characterized by an average Fe–O distance $\bar{L} = 2{\cdot}084$ Å. If we assume a linear relation between

TABLE III. *Julgoldite. Anisotropic temperature factors (from the expression* $\exp(h^2B_{11}a^{*2}/4 + \ldots + 2hkB_{12}a^*b^*/4 + \ldots))$. $\bar{\sigma}(B)$ *is the standard deviation averaged over all six or four varied* B_{ik}

Atom	B_{11}	B_{22}	B_{33}	B_{12}	B_{13}	B_{23}	$\bar{\sigma}(B)$
Ca(1)	0·64	0·64	0·30	0	0·08	0	0·05 Å²
Ca(2)	1·31	0·66	0·44	0	0·00	0	0·06
Fe(1)	1·07	0·74	0·52	0·03	0·12	0·05	0·04
Fe(2)	0·80	0·63	0·35	0·04	0·10	0·04	0·03
Si(1)	0·46	0·49	0·16	0	−0·06	0	0·07
Si(2)	0·66	0·39	0·19	0	−0·06	0	0·07
Si(3)	0·49	0·49	0·14	0	0·07	0	0·07
O(1)	1·14	0·66	0·46	−0·19	0·08	−0·16	0·15
O(2)	0·99	0·58	0·40	0·06	−0·05	−0·11	0·14
O(3)	1·18	0·84	0·51	0·16	0·25	0·14	0·15
O(4)	0·64	0·53	0·31	0	0·08	0	0·19
O(5)H	1·24	1·04	0·64	0	0·03	0	0·24
O(6)	0·94	0·38	0·27	0	0·05	0	0·20
O(7)H	1·26	0·81	1·04	0	0·24	0	0·24
O(8)	0·96	1·07	0·29	0	−0·06	0	0·22
O(9)	0·80	0·73	0·29	0	0·14	0	0·20
O(10)H	1·32	1·20	0·71	0	0·20	0	0·24
O(11)H	1·24	0·87	0·56	0	0·23	0	0·23

the $Fe^{2+}/(Fe^{2+}+Fe^{3+})$ ratio and the mean octahedral bond length, $\bar{L}$(Fe–O) (as we do, for example, when deriving the Al occupancy in (Si,Al) tetrahedra) we may predict the Fe(1) occupancy thus: from the effective ionic radii of Shannon and Prewitt (1969) [$r(^{vi}Fe^{2+}) = 0{\cdot}77$ Å, $r(^{vi}Fe^{3+}) = 0{\cdot}645$ Å and $r(^{vi}O^{2-}) = 1{\cdot}38$ Å], we calculate the expected values for pure Fe^{2+} and pure Fe^{3+} occupancy as $\bar{L}(Fe^{2+}\text{–}O) = 2{\cdot}15$ Å and $\bar{L}(Fe^{3+}\text{–}O) = 2{\cdot}025$ Å; for the measured value $\bar{L} = 2{\cdot}084$ Å, we obtain, by linear interpolation, an Fe(1) occupancy of $Fe^{3+}_{0{\cdot}52}Fe^{2+}_{0{\cdot}48}$.

For Fe(2), which occupies two-thirds of the octahedra, the experimental $\bar{L}$ value is 2·011 Å. Even if the three-fold coordination of O(1) and O(3), which are bonded to Fe(2), is considered, the expected $\bar{L}$ value for Fe(2) is 2·018 Å [$r(^{iii}O^{2-}) = 1{\cdot}36$ Å]. Therefore Fe(2) should be the site of Al substitution [$r(^{vi}Al) = 0{\cdot}53$ Å]. A replacement of 6% of Fe^{3+} by Al, indicated by the microprobe analysis (Table I, *c* and *d*), reduces the calculated $\bar{L}$ exactly to 2·011 Å.

The octahedral chains are joined in the *ac* plane by SiO_4 and $Si_2O_6(OH)$ groups, forming 5-membered rings of two octahedra and three tetrahedra. Half of the rings are open and have a Ca(1) ion at their centre; the other rings are closed and

TABLE IV. *Observed and calculated powder patterns of julgoldite*

I_{obs}*	I_{calc}	d_{obs}	d_{calc}	*hkl*	I_{obs}	I_{calc}	d_{obs}	d_{calc}	*hkl*
2	16	9·57(8) Å	9·631 Å	002	4	4	1·732(2)	1·741	415
2	18	8·82(7)	8·844	100		21		1·738	$42\bar{4}$
—	7	—	6·991	$10\bar{2}$		6		1·737	135
1	13	6·14(3)	6·123	102	1	4	1·715(2)	1·720	$3.0.\bar{1}\bar{0}$
—	9	—	4·940	$11\bar{1}$		6		1·718	406
7	58	4·80(2)	4·815	004	1	4	1·694(2)	1·696	513
	38		4·763	111		6		1·693	$1.1.\bar{1}\bar{1}$
—	11	—	4·486	$10\bar{4}$	2	10	1·673(2)	1·675	$33\bar{1}$
1	18	4·43(2)	4·422	200	$5\frac{1}{2}$	4	1·622(2)	1·627	0.2.10
—	6	—	4·237	$20\bar{2}$		54		1·621	424
—	6	—	4·102	$11\bar{3}$	1	19	1·605(2)	1·605	0.0.12
—	4	—	4·012	104	3	27	1·585(2)	1·586	$2.2.\bar{1}\bar{0}$
8	83	3·84(1)	3·831	202	—	5	—	1·569	1.2.10
—	15	—	3·495	$20\bar{4}$	—	11	—	1·531	408
—	4	—	3·451	211	$5\frac{1}{2}$	34	1·517(2)	1·520	040
1	16	3·059(8)	3·061	204		29		1·515	$42\bar{8}$
—	4	—	2·991	213	—	5	—	1·508	$52\bar{4}$
10	83	2·950(7)	2·949	115	2	17	1·472(2)	1·475	2.2.10
	17		2·948	300	1	6	1·429(1)	1·429	602
	20		2·929	$30\bar{2}$		5		1·428	$1.2.\bar{1}\bar{2}$
—	16	—	2·899	022	1	3	1·416(1)	1·419	0.2.12
—	16	—	2·875	120		6		1·413	242
6	10	2·778(7)	2·788	$12\bar{2}$		4		1·412	$60\bar{6}$
	68		2·778	$20\bar{6}$	2	9	1·390(1)	1·389	$4.0.\bar{1}\bar{2}$
3	13	2·717(6)	2·723	122	1	4	1·366(1)	1·367	428
	6		2·720	302		2		1·365	$43\bar{7}$
4	34	2·680(6)	2·671	$31\bar{1}$		2		1·365	$3.1.\bar{1}\bar{3}$
7	81	2·568(6)	2·571	024		2		1·363	$52\bar{8}$
—	9	—	2·517	$12\bar{4}$	—	2	—	1·353	435
4	19	2·491(5)	2·505	220		3		1·351	340
	24		2·492	$11\bar{7}$		3		1·349	$34\bar{2}$
—	21	—	2·470	$22\bar{2}$	$2\frac{1}{2}$	12	1·322(1)	1·336	$62\bar{2}$
$1\frac{1}{2}$	6	2·433(5)	2·448	206		14		1·334	$24\bar{6}$
	3		2·423	124		4		1·332	$53\bar{3}$
—	5	—	2·408	008		3		1·330	$1.3.\bar{1}\bar{1}$
	5		2·405	$10\bar{8}$	—	9	—	1·320	$62\bar{4}$
5	52	2·385(5)	2·382	222	1	3	1·281(1)	1·281	$62\bar{6}$
—	12	—	2·354	313		1		1·280	$43\bar{9}$
—	6	—	2·317	$31\bar{5}$		1		1·280	533
3	26	2·240(4)	2·243	$20\bar{8}$		3		1·277	606
1	5	2·209(4)	2·220	$40\bar{2}$	1	9	1·266(1)	1·267	2.0.14
	15		2·211	400		2		1·267	$1.1.\bar{1}\bar{5}$
	6		2·208	026	$1\frac{1}{2}$	5	1·252(1)	1·258	$24\bar{8}$
—	5	—	2·189	$12\bar{6}$		3		1·255	519
2	27	2·158(4)	2·157	224		5		1·253	0.2.14
2brd	16	2·121(4)	2·118	$40\bar{4}$		1		1·253	$6.0.\bar{1}\bar{0}$
	5		2·097	126		6		1·253	440
1	3	2·034(3)	2·035	$31\bar{7}$	—	5	—	1·235	$44\bar{4}$
1	3	1·959(3)	1·960	131	—	7	—	1·144	155
1	7	1·948(3)	1·945	$40\bar{6}$	—	10	—	1·119	0.2.16
2	17	1·902(3)	1·907	226	—	4	—	1·111	$15\bar{7}$
3	29	1·885(3)	1·888	028		6		1·110	$80\bar{4}$
	5		1·886	$12\bar{8}$	2	5	1·103(1)	1·105	800
	4		1·873	324		3		1·105	3.1.15
—	5	—	1·788	420		2		1·104	$72\bar{8}$
						18		1·104	0.4.12
						4		1·103	724

surround a Ca(2) ion. These same columns of 5-membered rings also form structural building blocks in epidote, zoisite, ardennite, ilvaite, etc.

Bond-valence sums and hydrogen bonds. In order to assign bond valences, v, to the experimentally determined interatomic distances, L (table V), we use the formula discussed above: $Ca_2(Fe^{3+}_{0\cdot52}Fe^{2+}_{0\cdot48})(Fe^{3+}_{0\cdot94}Al_{0\cdot06})_2Si_3O_{10\cdot52}(OH)_{3\cdot48}$. This formula contains 5·7 wt % H_2O, thus bringing the total for the analysis (table I, *c*) to 99·0 %.

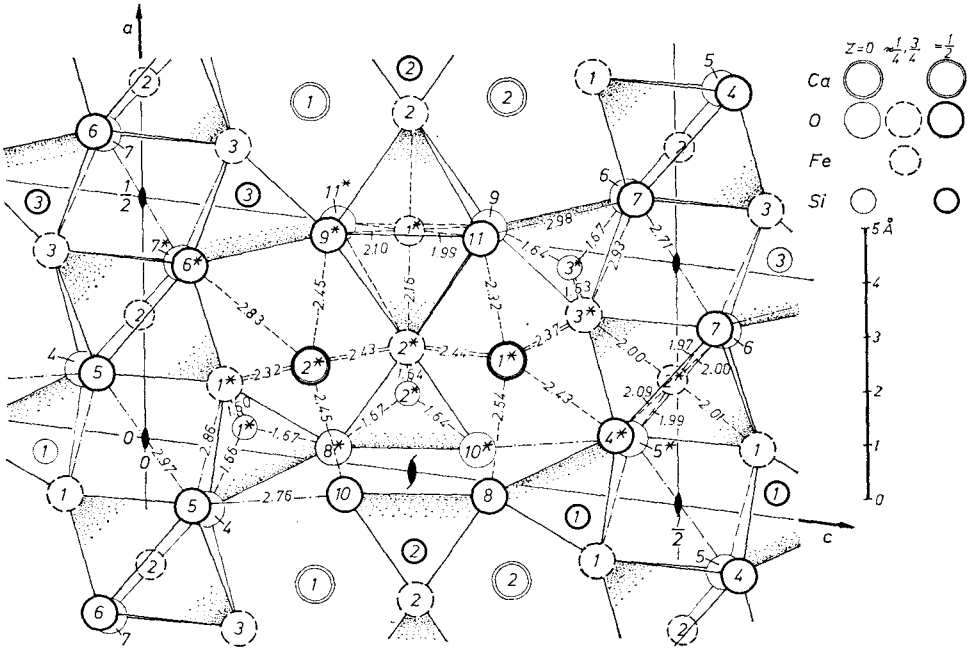

FIG. 1. Julgoldite crystal structure projected parallel to [010] onto (010). The origin is in the lower left-hand corner; a portion of the cell extending to about $\frac{1}{2}$ *a* and $\frac{1}{2}$ *c* is shown (–·–·– hydrogen bonds). An asterisk, *, indicates the site for which co-ordinates are listed in Table II.

The following relations, given in detail in Donnay and Allmann (1970), are used to calculate bond valences: $v = v_i \cdot (\bar{L}/L)^p$ for $L \leqslant \bar{L}$ and $v = v_i\,(L_{max}-L)/(L_{max}-\bar{L})$ for $\bar{L} \geqslant L \geqslant L_{max}$. The ideal valence v_i, the ratio of formal cation charge to cation coordination number, is thus assigned to the mean bond length L of every given cation polyhedron. In this way the relation of bond length to bond valence is tailored to fit each individual structure. For bonds longer than the mean, the relation used is linear, with the zero value of v assigned to 'L_{max}', the sum of the so-called maximum bonding

NOTE TO TABLE IV

* Observed data from the literature (Moore, 1971) taken with Fe/Mn radiation (σ (θ) assumed as 0·05°). Calculated data (E. Evans, private communication) based on Fe-$K\alpha$ radiation. I_{calc} is an integrated intensity based on $I(115)+I(300) = 100$. All $I_{calc} \geqslant 4\cdot0$ are listed out to $d_{min} = 1\cdot10$ Å.

TABLE V. *Bond lengths* (Å) *and bond valences* (v_i) *of julgoldite*, $Ca_2(Fe^{3+}_{0\cdot52}Fe^{2+}_{0\cdot48})(Fe^{3+}_{0\cdot94}Al_{0\cdot06})_2Si_3O_{10\cdot52}(OH)_{3\cdot48}$

Anions	Ca(1)	Ca(2)	Fe(1)	Fe(2)	Si(1)	Si(2)	Si(3)	$\Sigma_C v$
O(1)		2·324(6)		2·005(5)	1·605(6)			
		0·339*		0·507	1·061*			1·908
O(2)	2·439(6)	2·427(6)	2·155(5)			1·636(6)		
	0·276*	0·296*	0·333*			1·021*		1·927
O(3)	2·365(6)			2·002(5)			1·626(6)	
	0·302*			0·511			1·033*	1·847
O(4)	2·428(8)			2·095(7)	1·657(8)			
	0·280			0·389†	0·954			2·011
O(5)H				1·993(8)				
				0·524†				1·048
O(6)		2·826(8)		2·003(7)			1·673(8)	
		0·153		0·510†			0·936	2·109
O(7)H				1·969(8)				
				0·559†				1·117
O(8)	2·537(8)				1·672(8)	1·669(8)		
	0·243				0·924	0·953		2·119
O(9)		2·446(8)	2·103(7)				1·643(8)	
		0·289	0·392*†				0·998	2·072
O(10)H		2·453(8)				1·644(8)		(1·22 estim.)
		0·287				1·005		1·291
O(11)H	2·138(8)		1·993(8)					(1·30 estim.)
	0·320		0·534*†					1·389
$\bar{L}$	2·413	2·461	2·084	2·011	1·635	1·646	1·642	
L	3·250	3·250	2·448	2·390	2·130	2·130	2·130	
p	2·883	3·119	5·719	5·309	3·301	3·403	3·365	
v_i	2·00/7	2·00/7	2·52/6	3·00/6	4·00/4	4·00/4	4·00/4	
NF	0·998	0·993	0·987	0·998	0·999	1·000	1·000	
$\Sigma_A v$	2·000	2·000	2·520	3·000	4·000	4·000	4·000	
For comparison: $\bar{L}$ of pumpellyite								
	2·42	2·45	1·99	1·92	1·63	1·64	1·645	

* Two bonds per cation. † Two bonds per anion.

radii of cation and anion. These radii, r_{max}, are obtained by extrapolating v_i *vs* r to zero v_i (r refers to effective ionic radii given for different coordination numbers by Shannon and Prewitt, 1969). The exponential p, used to evaluate v for bond lengths less than the mean, is chosen so as to avoid a singularity in slope where the two curve fragments meet; thus its value is $p = \bar{L}/(L_{max}-\bar{L})$. Because of the non-linear relation on the short bond length side of $\bar{L}$, the $\Sigma_A v$ values for the cations need a slight normalization to the ideal charge values of the cations, as indicated by the normalization factors in the penultimate row of table V.

From the magnitude of anionic valence sums ($\Sigma_C v$, table V), we infer that O(5) and O(7), corners of the Fe(2) octahedron (fig. 1), are hydroxyl groups. The other two anions with valence sums closer to 1 than 2 are O(10) and O(11), of which the former represents the free corner of the Si(2) tetrahedron and the latter, a corner of the Fe(1) octahedron. The values of 1·29 and 1·39 valence units respectively leave no doubt that

the major occupants of these positions are hydroxyl groups, with some O^{2-}-for-OH^- substitution. It is rare to find a silicon tetrahedron with a hydroxyl group at a corner, and we are therefore not surprised that partial substitution of O for OH takes place at the O(10) position.

TABLE VI. *Lengths of edges of coordination polyhedra, angles subtended by edges at central cations, cation approaches, and possible hydrogen bond lengths.* (σ(O–O) $\leqslant$ 0·01 Å, $\sigma(\angle) \leqslant 0{\cdot}1°$)

around Fe(1)	*d*(O–O)	∠O–*Me*–O	around Si(1)	*d*(O–O)	∠O–*Me*–O
O(2)–O(9)	3·02 Å	90·2°	O(1)–O(1)	2·69 Å	114·0°
O(2)–O(9′)	3·01	89·8	O(1)–O(4)	2·69	111·2
O(2)–O(11′)	2·92	89·5	O(1)–O(8)	2·67	109·1
O(2)–O(11)	2·95	90·5	O(4)–O(8)	2·58	101·6
O(9)–O(11′)	2·73*	83·7			
O(9)–O(11)	3·05	96·3	around Si(2)		
			O(2)–O(2)	2·79 Å	116·8°
around Fe(2)			O(2)–O(8)	2·67	107·8
O(1)–O(4)	2·90 Å	90·1°	O(2)–O(10)	2·69	110·1
O(1)–O(5)	2·87	91·8	O(8)–O(10)	2·60	103·3
O(1)–O(6)	2·83	89·7			
O(1)–O(7)	2·75	87·5	around Si(3)		
O(3)–O(4)	2·85	88·1	O(3)–O(3)	2·67 Å	110·1°
O(3)–O(5)	2·77	87·7	O(3)–O(6)	2·71	110·4
O(3)–O(6)	2·88	92·1	O(3)–O(9)	2·72	112·5
O(3)–O(7)	2·88	92·9	O(6)–O(9)	2·55	100·8
O(4)–O(5)	3·05	96·5			
O(4)–O(7)	2·63*	80·8	around Ca(1) (< 3·3 Å)		
O(5)–O(6)	2·63*	82·4	O(2)–O(2)	3·29 Å	84·9°
O(6)–O(7)	3·05	100·3	O(2)–O(3)	3·25	85·1
			O(3)–O(3)	(3·42)	92·4
			O(3)–O(11)	2·93	77·3
Fe(1)–Fe(1)	3·041 Å				
Fe(2)–Fe(2)	3·083		around Ca(2) (< 3·4 Å)		
	2·998		O(1)–O(1)	3·39 Å	93·5°
Si(1)–Si(2)	3·031		O(2)–O(2)	3·29	85·5
Fe(2)–Si(1)	3·198				
Fe(2)–Si(3)	3·168		*d*(O–O) of possible hydrogen bonds		
Ca(1)–Si(1)	3·174				
			O(1) . . . O(5)	2·86 Å	
∠(Si(1)–O(8)–Si(2))	130·3°		O(3) . . . O(7)	2·93	
			O(5) . . . O(5′)	2·97	
			O(5) . . . O(10)	2·76	
			O(7) . . . O(7′)	2·71	
			O(7) . . . O(11)	2·98	

* Shared edge.

Next we investigate the oxygen–oxygen approaches below 3·1 Å (table VI) to see what hydrogen bonding is possible: 3·0 out of the 3·48 hydrogen atoms per formula unit can be placed between O(10)...O(5)...O(5′)...O(10′) and between O(11)... O(7)...O(7′)...O(11′) (for distances see table VI and fig. 1; for angles, table VII), both sets of atoms possessing a twofold symmetry axis. Because the bonds are too

large for symmetrical hydrogen bonds, the proton arrangement must be disordered as shown for the first group: O(10)–H...O(5)–H...O(5′)–H...O(10′) or O(10)... H–O(5)...H–O(5′)...H–O(10′). Because of this disordered arrangement, no net charge transfer occurs within these hydrogen bond chains.

TABLE VII. *Interbond angles at hydrogen bonded oxygen atoms*

Angles at O(1)		Angles at O(3)	
Fe(2)–O–Ca(2)	= 110·6°	Fe(2)–O–Ca(1)	= 101·9°
Fe(2)–O–Si(1)	= 124·3	Fe(2)–O–Si(3)	= 121·3
Fe(2)–O . . . H–O(5)	= 105·9	Fe(2)–O . . . H–O(7)	= 97·1
Ca(2)–O–Si(1)	= 122·6	Ca(1)–O–Si(3)	= 134·0
Ca(2)–O . . . H–O(5)	= 79·7	Ca(1)–O . . . H–O(7)	= 92·4
Si(1)–O . . . H–O(5)	= 98·8	Si(3)–O . . . H–O(7)	= 96·9
Angles at O(5)H		**Angles at O(7)H**	
Fe(2)–O–Fe(2′)	= 97·5°	Fe(2)–O–Fe(2′)	= 103·1°
*Fe(2)–O(5)–H . . . O(5′)	= 102·4(2×)	*Fe(2)–O–H . . . O(7′)	= 105·5(2×)
Fe(2)–O(5) . . . H–O(10)	= 114·9(2×)	Fe(2)–O . . . H–O(11)	= 118·4(2×)
O(5′)—H–O(5)...H–O(10)	= 121·3	O(7′)...H–O...H–O(11)	= 104·8
Angles at O(10)H†		**Angles at O(11)H**	
Ca(2)–O–Si(2)	= 144·5°	Ca(1)–O–Fe(1)	= 101·1°(2×)
Ca(2)–O–H . . . O(5)	= 79·8	Ca(1)–O–H . . . O(7)	= 92·3
Si(2)–O–H . . . O(5)	= 135·7	Fe(1)–O–Fe(1′)	= 99·4
		Fe(1)–O–H . . . O(7)	= 127·5(2×)

* The central atom is assumed to be the donor atom, which will be true in half the cases. The angles remain unchanged for the other case.

† Planar surrounding indicates sp^2 state for O(10).

If both O(10) and O(10′) (or O(11) and O(11′)) are hydroxyl groups (56 and 40% respectively of all cases), the above chains are impossible. In this case the 3-coordinated oxygen ions O(1) and O(3) are possible acceptor ions, judging by their distance from O(5)H and O(7)H respectively, but among the interbond angles that would be subtended at the latter hydroxyl ions, assuming linear hydrogen bonds, are Fe(2)–O(5)–H...O(1) of 160° and Fe(2)–O(7)–H...O(3) of 162°, which deviate too far from tetrahedral angles to be acceptable. The bifurcated hydrogen bonds

$$\mathrm{O(5)–H}\begin{cases}\cdots\mathrm{O(1)}\\ \cdots\mathrm{O(1')}\end{cases} \quad \text{and} \quad \mathrm{O(7)–H}\begin{cases}\cdots\mathrm{O(3)}\\ \cdots\mathrm{O(3')}\end{cases},$$

on the other hand, leave the hydrogen atoms on the mirror planes and reduce the above angles to 128°. Note that the high B values for the four hydroxyl groups (table II) may well be due to slight positional disorder of these atoms. A neutron-diffraction study is needed to test our predictions for the disordered hydrogen bonds.

Acknowledgements. We thank Professor. Paul B. Moore for donating the julgoldite sample and Mrs. Eloise H. Evans for calculating the powder pattern. Mr. Heinz P. Jepsen did the drawing of fig. 1. Most of the calculations were performed at the Rechenzentrum der Universität Marburg. Professor J. D. H. Donnay read the manuscript critically and gave much helpful advice.

REFERENCES

ALLMAN (R.) and DONNAY (GABRIELLE), 1971, *Acta Cryst.* **B27**, 1871–5.
COOMBS (D. S.), 1961. *Austral. Journ. Sci.* **24**, 203–15.
CROMER (D. T.), 1965. *Acta Cryst.* **18**, 17–23.
DONNAY (GABRIELLE) and ALLMANN (R.), 1970. *Amer. Min.* **55**, 1003–15.
GALLI (E.) and ALBERTI (A.), 1969. *Acta Cryst.* **B25**, 2276–81.
HANSON (H. P.), HERMAN (F.), LEA (J. D.), and SKILMAN (S.), 1964. Ibid. **17**, 1040–4.
—— and POHLER (R. F.), 1966. Ibid. **21**, 435.
MOORE (P. B.), 1971. *Lithos*, **4**, 93–9.
SHANNON (R. D.) and PREWITT (C. T.), 1969. *Acta Cryst.* **B25**, 925–46

[*Manuscript received 2 October 1972*]